Ceramics International 42 (2016) 9557–9564

Contents lists available at ScienceDirect

Ceramics International

journal homepage: www.elsevier.com/locate/ceramint

Fabrication of Ti_3SiC_2-based composites via three-dimensional printing: Influence of processing on the final properties

Mylena Mayara Matias Carrijo [a,b], Hannes Lorenz [a,*], Ina Filbert-Demut [a], Guilherme Mariz de Oliveira Barra [b], Dachamir Hotza [c], Xiaowei Yin [d], Peter Greil [a], Nahum Travitzky [a]

[a] Department of Materials Science, Institute of Glass and Ceramics, University of Erlangen-Nuremberg, 91058 Erlangen, Germany
[b] Department of Mechanical Engineering, Federal University of Santa Catarina (UFSC), 88040-900 Florianópolis, SC, Brazil
[c] Department of Chemical Engineering, Federal University of Santa Catarina (UFSC), 88040-900 Florianópolis, SC, Brazil
[d] Northwestern Polytechnical University, Science and Technology on Thermostructure Composite Materials Laboratory, Xi'an 710072, Shaanxi, People's Republic of China

ARTICLE INFO

Article history:
Received 26 January 2016
Received in revised form
29 February 2016
Accepted 4 March 2016
Available online 5 March 2016

Keywords:
A. Sintering
Cold isostatic pressing
Three-dimensional printing
Titanium silicon carbide
Uniaxial pressing

ABSTRACT

In this work the influence of the processing routes on the microstructure and properties of Ti_3SiC_2-based composites was investigated. The three main processing steps are (i) three-dimensional printing of Ti_3SiC_2 powder blended with dextrin, (ii) pressing of printed samples (uniaxial or cold isostatic pressing), and (iii) sintering of pressed samples at 1600 °C for 2 h. The Ti_3SiC_2-based composites were analyzed by X-ray diffraction (XRD), scanning electron microscopy (SEM), and energy-dispersive X-ray spectroscopy (EDS). Young's Modulus and flexural strength were measured to examine the mechanical properties. Porosity, density, shrinkage, and mass change were measured at each processing step. Those samples uniaxially pressed at 726 MPa presented the highest density, shrinkage, and mass change. However, microstructural morphologies were crack-free and homogeneous for cold isostatic pressed Ti_3SiC_2-based composites as compared to uniaxially pressed samples. The highest values for Young's Modulus (~300 GPa) and flexural strength (~3 GPa) were observed with uniaxially pressed Ti_3SiC_2-based composites.

1. Introduction

Titanium silicon carbide, Ti_3SiC_2, has attracted attention due to its unique combination of mechanical, electrical, and thermal properties of both metals and ceramics. As a result, it exhibits good thermal shock resistance, high electrical, and thermal conductivity, high oxidation and chemical resistance, easy machinability, low hardness, and high stiffness and Young's Modulus [1–5]. Ti_3SiC_2 can be synthesized from raw powders by chemical vapor deposition (CVD), combustion synthesis, reactive sintering, hot isostatic pressing (HIP), hot pressing, or spark plasma sintering [1,3,4,6,7].

Three-dimensional printing (3DP) emerged as a cheaper and faster alternative for the fabrication of three-dimensional parts compared to conventional powder consolidation techniques. 3DP consists of a plane, line or point addition of the desired material with the aid of a CAD-program, allowing for fabrication without the need of molds or die walls. The 3DP process is based on ink-jet printing technology, which has two approaches: direct and indirect. In direct ink-jet printing, a ceramic suspension in a volatile liquid is used as ink that is printed on an absorbent substrate. In the indirect ink-jet printing approach, the ink is a binder solution which is printed onto the powder layer. This ink is responsible for binding the powder layers one to another until the required part is completely finished [8,9]. One of the advantages of 3DP is the production of ceramic bodies with complex geometry with a low energy demand and without any toxic materials.

However, final parts produced via indirect 3DP may present a remaining porosity, which is influenced by particle size, layer thickness, and binder saturation [10]. Alternative processing steps as sintering, uniaxial, and cold isostatic pressing can be used to enhance the final density of printed samples. Ma et al. (Quelle [11]) recently fabricated MAX-phase-based ceramics by the combination of 3DP and reactive melt infiltration, which allows the manufacturing of compounds with complex shapes. Sun et al. [7] presented the properties of Ti_3SiC_2-structures after 3DP and cold isostatic pressing. In this work, the influence of both cold isostatic and uniaxial pressing after 3DP on density, shrinkage, mass change, microstructure, and mechanical properties on the final

* Corresponding author.
E-mail address: hannes.lorenz@fau.de (H. Lorenz).

http://dx.doi.org/10.1016/j.ceramint.2016.03.036
0272-8842/

parts was analyzed and compared to the work of Sun et al. [7].

2. Experimental

2.1. Powder mixture preparation

Ti_3SiC_2 powder (d_{50}=3 μm; Beijing Jinhezhi, China) with 2 wt% TiC and Ti_5Si_3 was blended with 10 wt% dextrin (Dextrin Superior Gelbmittel, Südstärke, Schrobenhausen, Germany), which was used as a binder. The powder was mixed for 48 h in a ball mill at room temperature. The Ti_3SiC_2 blended powder mixture was dried for 24 h at 70°C before 3DP.

2.2. Three-dimensional printing

For 3DP, an indirect 3D printer (ZPrinter® 310, Z Corp, Burlington, USA) was used, which implemented a design comprising a 2D profile with dimensions equal to $50 \times 7 \times 6$ mm^3 drafted in a CAD-program (SolidWorks 2010, Dassault Sistêmes SolidWorks, Concord, USA). The printer solution with 1:7 volume ratio of glycerin and distilled water was injected into a Ti_3SiC_2-blended powder bed. The thickness of the layer was 0.1 mm and binder saturation was 100% and 50% (shell/core). The printed samples were dried in two steps in the powder bed, first at room temperature for 24 h and later at 70 °C for 24 h.

2.3. Cold isostatic pressing (CIP) and uniaxial pressing

The printed samples were divided in 3 sets (Fig. 1). One sample set was uniaxially pressed under 726 MPa before sintering. Another sample set was subdivided in other three sets, which were pressed cold isostatically (CIP) at 35 MPa, 150 MPa, and 180 MPa prior to sintering. The last sample set was sintered without pressing and used for comparison.

For CIP, printed samples were first vacuum encapsulated in a latex bag and then in an aluminum bag. The aluminum bag was used to ensure adequate encapsulation of the samples because of the better stability compared to the latex bag during this process. After encapsulation, the samples were placed into a wet bag press machine (LOOMIS PRODUCT Kahlefelg, Kaiserslautern, Germany). The three subdivided sample sets were separated and pressed at 35, 150 and 180 MPa for 30 s.

For uniaxial pressing, the printed samples were subjected to a pressure of 726 MPa for 30 s in a uniaxial steel die of 6×50 mm^2 (Paul Otto Weber, Remshalden, Germany).

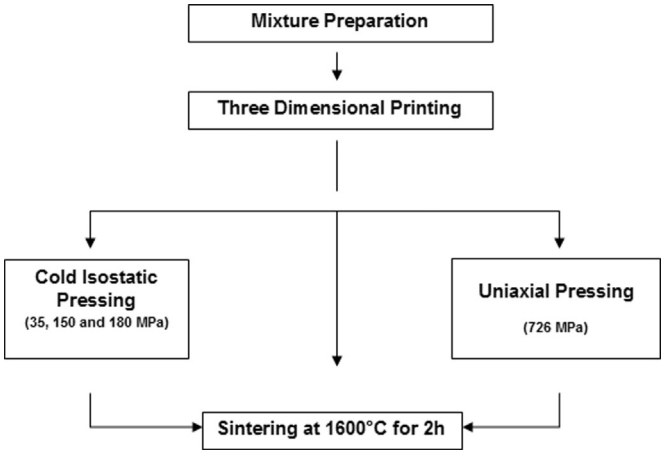

Fig. 1. Scheme of general experimental procedure.

2.4. Sintering

The three sample sets (as-printed, cold isostatic, and uniaxially pressed) were sintered in an alumina crucible which was placed in an alumina tubular furnace (HTRH 1000-300/18 GERO, Neuhausen, Germany) at 1600 °C performed in flowing argon atmosphere. The dwell time was 2 h and the heating and cooling rates were 180 K/h.

2.5. Characterization

The density, porosity, mass change and shrinkage were measured in each step of processing. The open porosity was calculated by using Eq. (1).

$$P_{open} = (1-(\rho_{geo}/\rho_{th}))\cdot 100 \quad (1)$$

where P_{open}=open porosity (%), ρ_{geo}=geometrical density (g/cm^3), ρ_{th}=theoretical density (g/cm^3). The actual density was measured by a helium-pycnometer (Accupyc 1330 Micromeretics, Norcross, USA) and the geometric density is the ratio of the mass (m) and volume (V) of the samples.

The shrinkage was calculated by using Eq. (2) according to changes in length (Δy), width (Δx), height (Δz) and volume (ΔV).

$$\Delta x = 100\cdot(X_{initial} - X_{final})/X_{initial} \quad (2)$$

The microstructure was examined by scanning electron microscopy (SEM; Quanta 200, FEI, Prag, Czech Republic). The chemical phase analysis of sintered and post-polished samples was evaluated by Energy-dispersive X-ray spectroscopy (EDX, INCA x-sight TVA3, Oxford Instruments, Oxford, UK).

Thermogravimetric analysis (TGA) and differential thermal analysis (DTA) were performed to investigate the thermal behavior of dextrin powder and Ti_3SiC_2-based composites after printing. The measurements were carried out in flowing argon with a heating rate of 300 K/h.

The effective Young's Modulus of sintered samples was measured with an ultrasonic measuring device (Krautkrämer, Hürth, Germany) according to DIN EN 843-2. The propagation time of a longitudinal wave in the sample was defined and the resonance peaks in horizontal and vertical directions of the samples were measured as showed in Eqs. (3) and (4).

$$E_h = (\varphi\cdot(l/t_h)^2\cdot(1+\nu)\cdot(1-2\nu))/(1-\nu) \quad (3)$$

$$E_v = (\varphi\cdot(l/t_v)^2\cdot(1+\nu)\cdot(1-2\nu))/(1-\nu) \quad (4)$$

where E_h=Young's Modulus in horizontal direction (MPa); E_v=Young's Modulus in vertical direction (MPa); l=length of sample (mm); h=height of sample (mm); t_h=resonance peak in horizontal direction (μm); t_v=resonance peak in vertical direction (μm); ν=Poisson ratio (0.2); ϕ=real density (g/cm³).

A four-point bending setup (DIN EN 843-1, 2008) was used to obtain the flexural strength by using an universal testing machine (Instron 5565, Carton, USA). Bending strength of the testing bars with dimensions of $30 \times 4 \times 5.5$ mm^3 were measured by 4-point bending method using spans of 10 mm and 20 mm. The speed of the crosshead was set up to 0.5 mm/min. The tensile surfaces of the samples were polished to a 6 μm diamond finish prior to bending.

3. Results and discussion

Fig. 2 illustrates the mass change after pressing for all specimens. Samples that underwent cold isostatic and uniaxial pressing